Surfaces and Interfaces 72 (2025) 107302

Contents lists available at ScienceDirect

Surfaces and Interfaces

journal homepage: www.sciencedirect.com/journal/surfaces-and-interfaces

Chitosan/polyacrylonitrile composite nanofibers for humidity sensing

Jialin Liu [a,b], Yuxuan Zhang [a], Wang Qin [a], Xiaowang Lu [c], Yanhua Cai [d], Junfeng Cheng [a], Chunlin Liu [a,b], Louis C.P.M. de Smet [e,*], Zheng Cao [a,b,*]

[a] Jiangsu Key Laboratory of Environmentally Friendly Polymeric Materials, School of Materials Science and Engineering, Jiangsu Collaborative Innovation Center of Photovoltaic Science and Engineering, Changzhou University, Changzhou 213164, Jiangsu, , PR China
[b] Changzhou University Huaide College, Jingjiang 214500, PR China
[c] School of Material Science and Engineering, Yancheng Institute of Technology, Yancheng, 224051, PR China
[d] Chongqing Key Laboratory of Environmental Materials & Remediation Technologies, Chongqing University of Arts and Sciences, 402160, Chongqing, PR China
[e] Advanced Interfaces & Materials, Laboratory of Organic Chemistry, Wageningen University, Stippeneng 4, 6708 WE Wageningen, The Netherlands

ARTICLE INFO

Keywords:
Humidity sensor
QCM
Chitosan
Polyacrylonitrile
Electrospinning

ABSTRACT

A coating of polyacrylonitrile (PAN) nanofibers was prepared onto gold-coated quartz crystal microbalance (QCM) sensors using an electrospinning method. Different deposition amounts of these nanofibers were obtained by controlling the deposition time. Subsequently, chitosan (CS) was spin coated onto these modified QCM sensors to obtain coatings of CS-PAN composite nanofibers. The resulting construct was employed as a QCM humidity sensor. Scanning electron microscopy (SEM), atomic force microscopy (AFM), laser scanning confocal microscopy (LSCM), and Fourier transform infrared spectroscopy (FT-IR) were used to characterize CS-PAN composite nanofibers in terms of their surface structure, morphology, roughness, dispersion, and composition. The humidity sensing characteristics of the CS-PAN composite nanofibers were studied in detail by QCM. The CS-PAN composite nanofiber modified QCM sensor responds strongly and reversibly to humidity, with a maximum frequency response of -1470 Hz (11–98 % RH), a high fitting correlation coefficient ($R^2 = 0.9998$), and a fast response/recovery time of < 4 s/33 s and 21 s/63 s at low and high humidity level, respectively. In addition, the QCM sensor based on CS-PAN nanofibers show high selectivity, high repeatability and long-term stability. The two-step electrospin/spin-coating fabrication of the high-correlation CS-PAN humidity sensor is not only facile and cost effective, but also versatile in terms of nanofiber functionalization.

1. Introduction

Humidity detection and control plays an increasingly important role in current daily life, industrial processing, and agricultural production, such as medical diagnosis, respiratory monitoring, meteorology, semiconductor industry, and food storage [1–5] The rapidly growing demand for humidity sensing has inspired many researchers to develop high-performance, electronic humidity sensors. A variety of humidity sensors (including those based on resistance [6], impedance [7], capacitive [8], modes of working) and sensing materials (including semiconductors, ceramics, carbon nanotubes [9], and organic polymers [10–13]) with different sensing methods have been developed. Among these approaches are interdigital electrodes (IDEs), sandwich capacitors, surface-acoustic-wave resonators (SAW), thin film bulk acoustic resonators (FBAR), capacitive micromachined ultrasonic transducers (CMUTs), and quartz crystal microbalance (QCM) [14–17] QCM is considered to be a strong candidate for the development of high-performance humidity sensors due to its low cost, high stability, and nanogram-level mass sensing capabilities [18,19] QCM is an extremely sensitive detection instrument to surface and interfacial mass changes with a high level of accuracy. Interestingly, QCM can also achieve real-time detection and making it widely used in interfacial studies in the field of chemistry, physics, biomedicine, and environmental science [20–32]

The design and selection of moisture-sensitive materials is key in determining the performance of QCM humidity sensors. A large number of studies have confirmed that the hydrophilicity and specific surface area of sensitive materials are the key factors affecting the sensitivity and stability of QCM humidity sensitive sensors. In recent years, researchers have developed many types of moisture-sensitive materials, including ceramics [33], metal oxides [34,35], carbon materials [36], and organic composites [37,38] Polymers are particularly interesting

* Corresponding authors.
E-mail addresses: louis.desmet@wur.nl (L.C.P.M. de Smet), zcao@cczu.edu.cn (Z. Cao).

https://doi.org/10.1016/j.surfin.2025.107302
Received 4 April 2025; Received in revised form 15 July 2025; Accepted 28 July 2025
Available online 28 July 2025

due to their remarkable diversity and flexibility in both structure and function. Additionally, their low cost and the ease with which their chemical and physical properties can be controlled across a wide range—through (co)polymerization, grafting, and surface modification—further enhance their value. Moreover, the selectivity and sensitivity of polymer films can be further tuned and boosted by functionalization strategies.

Polymer-based affinity coatings have been widely used in various gas sensors, humidity sensors, ion sensors and biosensors [3,39–45] For example, Liu *et al.* sprayed a suspension containing chitosan and polypyrrole onto a QCM sensor to obtain a composite CS/PPy film, which resulted in an effective humidity sensor in the range of 0–97 %RH [3] The hydrophilic structure of the affinity coating, combined with its incomplete coating structure, were reported to be relevant for the coating performance. Alternatively, Rianjanu *et al.* obtained a porous structure by electrospinning polyacrylonitrile (PAN) nanofiber onto a QCM sensor, which were then modified with polyethylenimine (PEI) by means of drop casting to increase the hydrophilicity [39] This humidity sensor showed a high sensitivity (164 Hz/ % RH) and high repeatability in the range of 33–75 % RH.

However, compared to ceramics and metal oxides, affinity coatings based on polymer films may suffer from poor mechanical properties and changes in their viscoelastic properties upon moisture absorption, which may negatively affect measurement results and sensor stability over prolonged times [40] The introduction of crosslinks, increased stiffness and/or inorganic materials into the polymer film may overcome such problems. For example, Yang *et al.* used natural polymers to prepare a series of green microspheres, including sodium alginate/polyglutamic acid (SA/PGA), sodium alginate/sodium hyaluronate (SA/HA), sodium alginate/sodium carboxymethyl cellulose (SA/CMC) by an emulsification/internal gel method [41] The resulting stiff materials were deposited on the surface of QCM sensors by drop casting and explored for their use in humidity and respiratory monitoring. They found that SA/PGA had the best sensing performance in the environment of 11–97 % RH, and had an increased recycling and reuse property. In a composite-based approach, Yuan *et al.* deposited graphene oxide/polyethylenimine (GO/PEI) layered film on QCM sensors via spraying, which was applied to humidity detection and found to have good moisture sensitivity characteristics [42] Zheng *et al.* fabricated a QCM-based humidity sensor based on a composite of polyvinyl alcohol/nano silica (PVA/-SiO_2), which showing a response to humidity as fast as 5s/21 s in a highly linear fashion within the range of 11–85 % RH [43] Wu *et al.* prepared a QCM humidity sensor based on graphene oxide (GO)-doped composite hydrogel, and found that the sensor had different frequency responses in different humidity environments [44]

While these examples show different approaches employed in the development of affinity coatings, they also show complicated preparation process, high material cost, and insufficient prominence of correlation coefficients. Chitosan (CS), as a natural polysaccharide polymer, contains hydrophilic groups such as hydroxyl groups and amino groups, which can be interact with water molecules under the action of hydrogen bonding, making it an attractive candidate to prepare a humidity affinity coating. At the same time, it has characteristics that enable easy film formation, high biocompatibility, and low production cost [46–48] However, dense polymer humidity sensor materials have the disadvantage of low sensitivity and long response/recovery time in the full humidity range. Electrospinning is a common method for changing the micromorphology of polymers, and polymer nanofibers with larger specific surfaces can be easily and rapidly produced [39, 49–51]

It is well-established that combining nanofibers with hydrophilic polymers like chitosan enhances the sensitivity of QCM sensors. Similar strategies employing different materials have been previously documented to improve surface area and molecular adsorption. Examples include polyaniline (PANi)-coated polyvinyl acetate (PVAc) nanofibers [52], Bamboo cellulose (BC)-coated PAN nanofibers [53], PVAc nanofibers coated with maltodextrin [54,55], and electrospun PAN nanofibers mixed with citric acid (CA) [56]

It is important to note that the use of electrospun nanofibers combined with chitosan rich in functional groups as an effective sensing coating for QCM humidity sensors builds further on existing work exploring similar composite structures [57,58] In this study, we fabricated a CS/PAN composite humidity-sensitive coating on a QCM sensor by 1) optimizing the electrospinning process parameters (specifically, deposition time) to control the deposition morphology of the PAN fiber layer, and 2) subsequently spin-coating CS solutions of varying concentrations. The influence of PAN deposition amount and CS coating quantity on sensing performance was systematically investigated to identify the composite structure with optimal humidity response characteristics.

Furthermore, while previous work primarily relies on QCM frequency changes alone to elucidate interactions between nanofibers/CS and molecules, our approach simultaneously utilizes both the QCM frequency shift (Δf) and half-band-half-width ($\Delta\Gamma$) shift. This dual-parameter analysis allows one to reveal concurrent changes in mass and viscoelastic properties of the CS-PAN nanofibers upon water molecule adsorption. Therefore, in this work, the low-cost and easily available PAN electrospun nanofibers were introduced into the CS humidity sensing system to obtain a CS-PAN composite, moisture-sensitive layer. Due to their good mechanical stability, PAN nanofibers can provide a stable rigid support for CS, reducing the energy dissipation caused by the rise of viscoelasticity of CS after water absorption, while increasing the specific surface area of CS. The sensing property, sensitivity, repeatability, and selectivity of QCM humidity sensor based on CS-PAN composite nanofibers, as well as its sensing mechanism, were studied.

2. Experimental section

2.1. Materials

Chitosan (CS, degree of deacetylation $\geq$ 95 %, the viscosity is between 100 and 200 mPa·s) and polyacrylonitrile (PAN, P30T) were purchased from Shanghai Zeye Biotechnology Co., Ltd., and Suzhou Huihuang Fluoroplasticizing Co., Ltd., respectively. *N,N*-dimethylformamide (DMF), concentrated sulfuric acid (H_2SO_4), hydrogen peroxide, acetic acid, deionized water, lithium chloride (LiCl), magnesium chloride ($MgCl_2$), magnesium nitrate ($Mg(NO_3)_2$), sodium chloride (NaCl), potassium chloride (KCl), and potassium sulfate (K_2SO_4) are all of analytical pure and purchased from Sinopharm Chemical Reagent Co., Ltd (Shanghai, China). QCM sensors (5 MHz, AT-cut quartz crystal coated with gold electrode) were purchased from Suzhou Siju Biomaterials Co., Ltd., Suzhou, China.

2.2. Cleaning of QCM sensor

Before each QCM experiment, QCM sensors were soaked in piranha solution, i.e., a mixture of concentrated sulfuric acid and hydrogen peroxide [25 %] with volume ratio of 7:3 (CAUTION: Piranha solution reacts violently with organic matter; it is important to prepare the solution in glassware that is free of any organic solvent and also by adding by adding hydrogen peroxide to sulfuric acid slowly, not the other way around!) for 15 min to remove any residues on the gold surface of QCM sensor. After the sensor was taken from the solution, it was rigorously rinsed with deionization water, before further rinsing it was ethanol and deionization water (3 ×), and finally drying it in a stream of high-purity nitrogen. Cleaned QCM sensor were stored in a closed container until their use in a QCM experiment.

2.3. Preparation of PAN nanofibers on QCM sensor

Fig. 1 shows a schematic illustration of the preparation of CS-PAN composite nanofibers and the QCM sensor modified with CS-PAN for

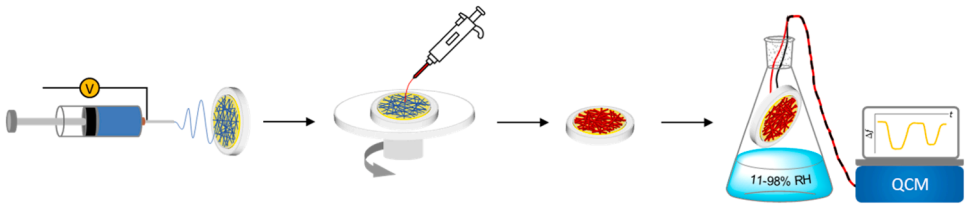

Fig. 1. Scheme illustrating the different steps of the preparation of a PAN (blue) nanofiber coating via electrospinning onto a QCM sensor, the subsequent deposition of CS (red) via spin coating to obtain a CS-PAN composite-coated QCM sensor, which is then used as a humidity sensor.

humidity test. First, PAN was dissolved in DMF, and then stirred for 6 h for ensure complete dissolution. After stirring, this solution was then left to stand for 3 h to eliminate bubbles, and was used to prepare PAN spinning solution with a concentration of 10 % (w/w). The PAN solution was then transferred to a 10 mL plastic syringe, which was mounted in a electrospinning machine (QZNT-E01, Foshan Nanofiberlabs Co., Ltd., Guangzhou, China). The QCM sensor was fixed on the collection roller of this device, and subsequently PAN nanofibers were deposited on the gold surface of the QCM sensor (Fig. 1, top left). The following spinning parameters were applied: a DC voltage of 20 kV, a distance of 15 cm between the nozzle and the collection roller, a syringe pushing speed of 1 mL/h, and a collection roller speed of 300 r/min. After the deposition of PAN fibers was completed (deposition times were 30 s, 60 s, 90 s, 120 s, respectively), the modified QCM sensors were dried in a vacuum drying oven at 60 °C for 12 h to remove any residual solvent.

2.4. Modification of PAN nanofibers with CS

In order to increase the affinity of the sensing layer for water molecules, the PAN nanofibers on the surface of QCM sensor were modified by spin-coating a CS solution using a spin-coating machine (KW-4A, Institute of Microelectronics, Chinese Academy of Sciences, China). A certain amount of CS powder was dissolved with 2.5 vol. % acetic acid solution and the obtained mixture was stirred for 6 h at room temperature. Light-yellow, transparent CS solutions were prepared with different concentrations of 0.5 wt. %, 1 wt. %, 1.5 wt. %, 2 wt. % and 2.5 wt. %, respectively. The CS solution volume for spin coating was set to be 100 μL. After spin coating, the QCM sensor modified with nanofibers was dried in vacuum at 60 °C for 6 h to remove the residual liquid on the sensor surface.

2.5. Humidity sensing settings

Different supersaturated saline solutions were used to provide different relative humidity environments for the humidity tests. Lithium chloride ($LiCl_2$), magnesium chloride ($MgCl_2$), magnesium nitrate ($Mg(NO_3)_2$), sodium chloride (NaCl), potassium chloride (KCl), potassium sulfate (K_2SO_4) supersaturated solutions provide an environment of about 11 % RH, 33 % RH, 55 % RH, 75 % RH, 86 % RH, 98 % RH in jars, respectively [59,60] The sensing test was performed at room temperature (~25 °C), and a QCM sensor coated with a coating of CS-PAN composite nanofibers as moisture-sensitive sensing material was placed in a QCM module and connected to a quartz crystal oscillator. Taking an 11 % RH humidity environment as the basic humidity environment, the moisture sensitivity characteristics of the CS-PAN nanofiber QCM humidity sensor were determined by recording the resonance frequency shift (Δf) caused by the change in mass load due to water molecules upon the adsorption by the moisture sensing layer on the gold electrode surface of the QCM sensor under different relative humidity environments.

To correlate the changes in oscillation frequency with changes in mass the Sauerbrey equation (Eq. (1)) was applied [61]:

$$\Delta m = \frac{-C\ \Delta f_n}{n} \quad (1)$$

where Δm is the area mass density of the absorbing film (mass per unit area, ng/cm^2), C is 17.7 ng·cm^{-2}·Hz^{-1}, with an effective area for the QCM sensor of 1.54 cm^2, and Δf_n is the frequency shift at the harmonic number n ($n = 1, 3, 5,\ldots$).

2.6. Material characterization

The fiber diameter, surface structure, morphology, and roughness of the moisture sensing layer were observed by high-resolution scanning electron microscopy (SEM, JSM-6360LA, JEOL, Japan), atomic force microscopy (AFM, Dimension Edge, BRUKER), and laser confocal microscopy (LSCM, Mahr MarSurf CM). A Fourier transform infrared spectrometer (FT-IR, Thermo Nicolet iS10, USA) was used to acquire FT-IR spectra of CS-PAN composite nanofiber coatings in the range of 4000–500 cm^{-1} at a resolution of 0.4 cm^{-1}. The moisture-sensitive characteristics and humidity responses of various CS-PAN nanofiber sensitive films were detected by iQCM equipment (Model QCM-A DBY-17, Hangzhou Longqin Advanced Materials Sci. & Tech. Co., Ltd., Hangzhou, China). X-ray diffraction (XRD) patterns were obtained by a X-ray diffractometer (D/max 2500 PC, Rigaku, Japan). Thermogravimetric (TG) and derivative thermogravimetric (DTG) curves were measured by a Thermogravimetric Analyzer (SDT Q600, TA, USA).

3. Results and discussion

3.1. Morphology and structure of cs-pan nanofibers

Fig. 2 shows SEM images of CS-PAN nanofibers with 2 wt. % CS at PAN electrospinning times of 30 s, 60 s, 90 s, 120 s. All modified surfaces showed a fiber structure with fiber lengths up to dozens, even up to hundreds of microns. From these images an average fiber diameter of 294 ± 90 nm was obtained (Fig. S1), resulting an aspect ratio of about to >100:0.29. This dimensional result is consistent with typical electrospun fiber diameters reported in the literature, which commonly fall between ~100 and ~800 nm [57,62] Furthermore, the amount of deposited fiber on the surface increased significantly with the electrospinning time. The controlled deposition of CS onto the coating of PAN fibers is aimed to provide a high-surface, hydrophilic affinity coating, providing adsorption sites for water molecules when exposed to humidity environment.

Fig. 3 shows SEM images of PAN fibers before (a, a') and after (b, b') spin coating CS at the PAN electrospinning time of 90 s. From Fig. 3, it can be observed that the surface of the bare PAN fibers (a, a') is scaly and not smooth, and after spinning CS (b, b'), it can be clearly seen that CS is coated on the surface of the fiber. In addition, the surface smoothness of the fibers is significantly improved, while after spinning CS, PAN can still maintain its fibrous shape, and the overall morphology has a certain stability. During coating fabrication, the CS solution was uniformly dispersed onto the nanofiber-coated QCM surface using a micropipette. A two-step spin-coating procedure was employed: an initial low-speed coating (500 rpm, 15 s) step facilitated solution infiltration into the fiber network, ensuring complete wetting of PAN surfaces. Subsequent high-speed coating (2000 rpm, 45 s) expelled excess solution along the fiber axis while forming a uniform residual film. A SEM image of an

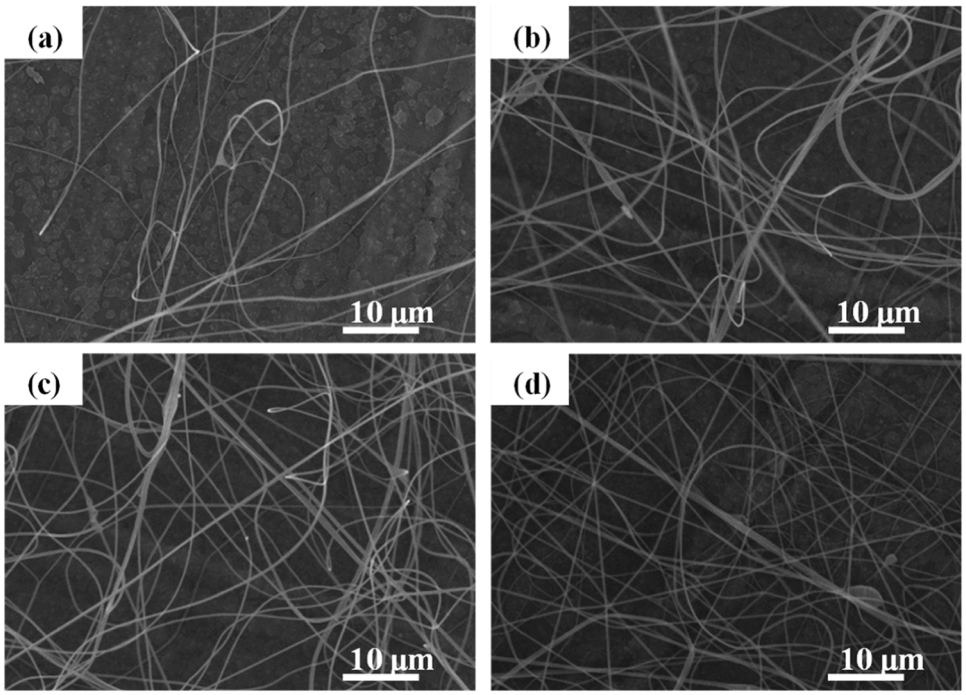

Fig. 2. SEM images of CS-PAN nanofibers with 2 wt. % CS at different PAN electrospinning times: (**a**) 30 s, (**b**) 60 s, (**c**) 90 s, (**d**) 120 s.

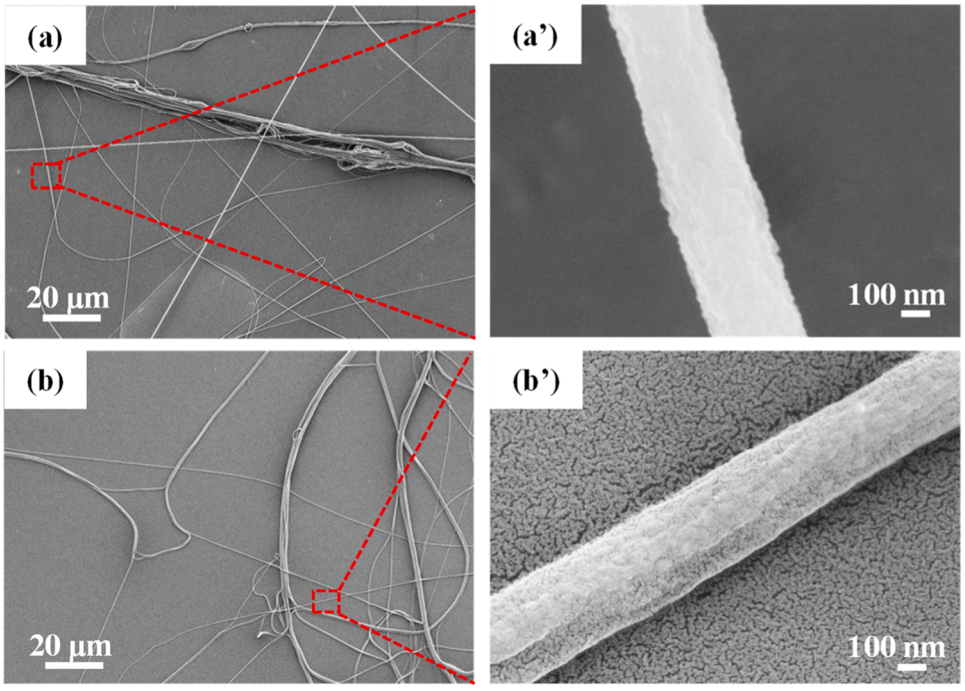

Fig. 3. SEM images of PAN fibers (prepared with an electrospinning time of 90 s) before (**a, a**') and after (**b, b**') spin-coating CS.

individual CS-PAN nanofiber (Fig. S2) reveals a smooth surface without aggregates, confirming homogeneous chitosan dispersion within the nanofibrous architecture.

Fig. 4 shows AFM maps of (3D and 2D cross-sectional profile, scanning area: 10 μm × 10 μm) CS-coated PAN nanofibers at different CS concentrations of 0.5 wt. %, 1 wt. %, 1.5 wt. %, 2 wt. %, and 2.5 wt. %. From Fig. 4, it can be seen that the CS-PAN composite fiber sensing layer has a three dimensional (3D) porous nanostructure. From the cross-sectional profiles of these samples, it can be seen that all CS-PAN composite nanofibers exhibit only slight contour differences with undulations of around 1 μm. Fig. 4f presents AFM maps of pure PAN nanofibers. It is noteworthy that the CS-coated PAN nanofibers largely retained a fibrous morphology, showing no significant structural alteration compared to the pristine PAN nanofibers. Based on the SEM and AFM results, the deposition of different concentrations of CS onto PAN nanofibers will not influence their 3D porous nanostructure.

Fig. 5 shows confocal laser scanning microscope images of pure CS and PAN nanofibers deposited with different concentrations of CS including 0.5 wt. %, 1 wt. %, 1.5 wt. %, 2 wt. %, and 2.5 wt. %. For all these samples a surface area of 257 × 257 μm[2] was scanned, and the

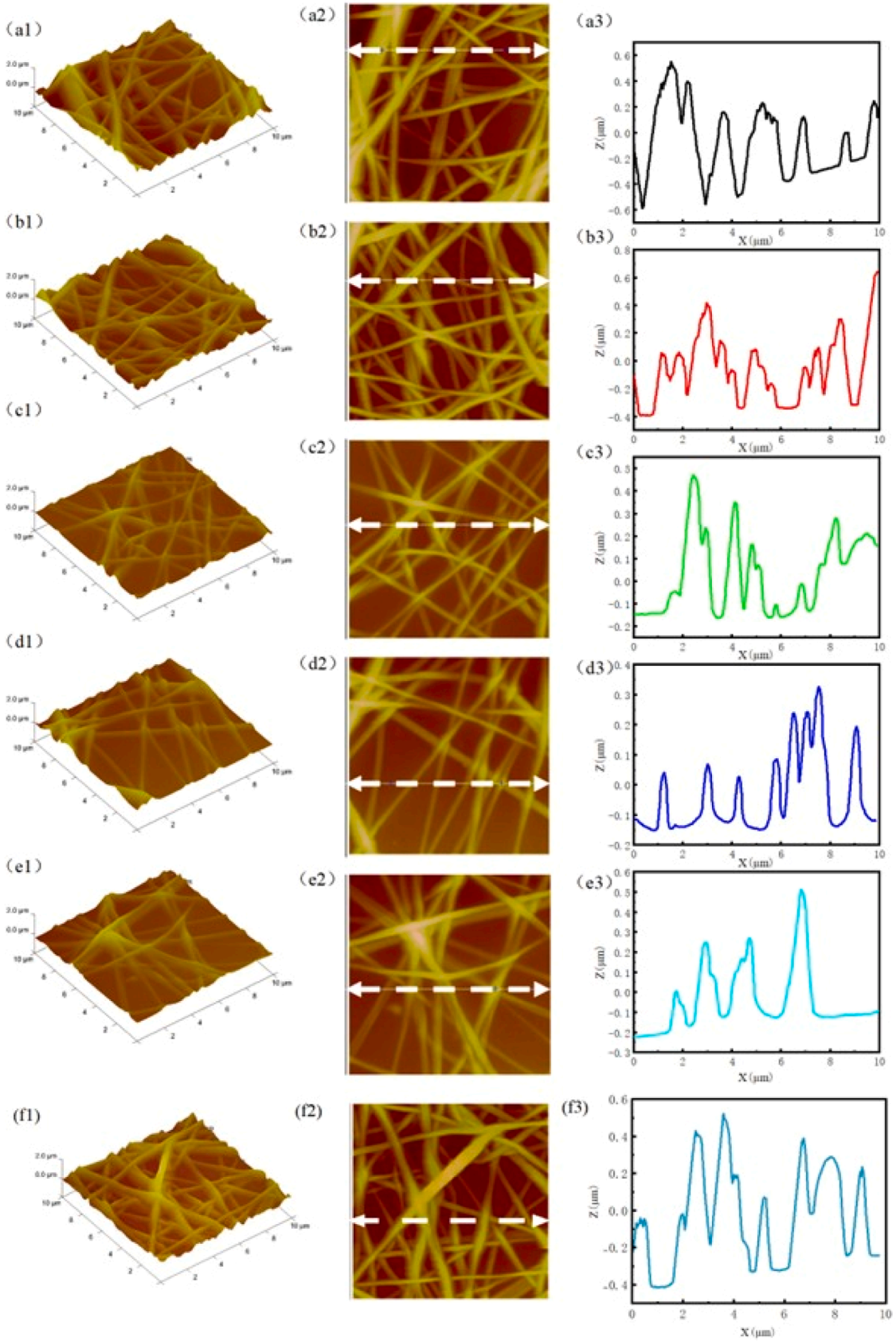

Fig. 4. AFM maps of (3D and 2D cross-sectional profile, scanning area: 10 μm × 10 μm) CS-coated PAN nanofibers at different CS concentrations: (**a**) 0.5 wt. %, (**b**) 1 wt. %, (**c**) 1.5 wt. %, (**d**) 2 wt. %, (**e**) 2.5 wt. %, and pure PAN nanofibers.

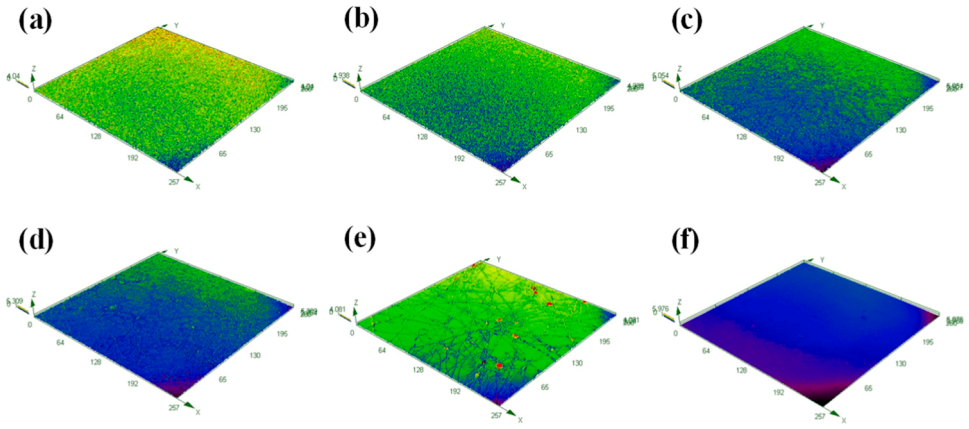

Fig. 5. Confocal laser scanning microscope images of PAN nanofibers (scanning area: 257 μm × 260 μm) deposited with different concentrations of CS including (**a**) 0.5 wt. %, (**b**) 1 wt. %, (**c**) 1.5 wt. %, (**d**) 2 wt. %, (**e**) 2.5 wt. %. and pure CS (**f**).

root mean square (RMS) values of the surface roughness were obtained according to the test results of LSCM. It was found that as the concentration of the spin-coated CS solution increased from 0.5 wt. % to 2.5 wt. %, the RMS value of CS-PAN composite nanofibers gradually decreased, i.e. from 572, 559, 383, 359 to 343 nm, respectively. The RMS value of pure CS coating is 151 nm. A possible explanation for this trend is that with the increase of the concentration of CS solution, the deposition amount of CS on the PAN nanofibers after spinning increases, and a large number of CS molecular chains fill the three-dimensional network structure of the PAN nanofibers, leading to the decreased surface roughness of the PAN nanofiber sensing layer. However, compared with the pure CS coating, the surface roughness of the CS-PAN nanofiber sensing layer significantly improved, and the rough surface is more conducive to improve the specific surface area of the sensing layer and providing more binding sites for water molecule adsorption. The analysis so far shows that the physical deposition of hydrophilic CS chains onto the surface of the electrospun PAN nanofiber does not significantly change the fiber structure, and at the same time, it also increases the roughness of the CS layer and the specific surface area of the whole PAN nanofiber layer.

In order to facilitate comparisons between sensor configurations quantitative estimates of the mass loading were made for the different samples. The approach entailed initially measuring the resonance frequency of a bare quartz crystal sensor in air to establish a baseline. Subsequently, the resonance frequency shift (Δf) was measured after depositing either CS or the CS-PAN composite onto the QCM sensors. The mass (Δm) deposited on the crystal surface was then calculated using Equation 1[61] The resulting mass loadings for the different samples are presented in Table 1. The combination of a 2.5 wt. % CS solution and a deposition time of PAN nanofibers of 90 s resulted in mass loading of 0.112 mg, which is line with functional coating loadings in comparable studies [53] Overall, the mass loading on the quartz crystal surface can be precisely controlled by adjusting the electrospinning time and CS mass fraction.

Table 1
Mass loadings per QCM sensor of different humidity-sensitive layers.

wt % CS	PAN electro-spinning times (s)	Mass (μg)
2	30	52 ± 2
2	60	87 ± 3
2	90	112 ± 3
2	120	129 ± 4
0.5	90	98 ± 2
1	90	105 ± 3
1.5	90	108 ± 5
2	90	112 ± 3
2.5	90	115 ± 2

Fig. 6 shows the FT-IR spectra of CS, PAN, and CS-PAN composite nanofibers, respectively. The FT-IR spectrum of CS has a wide and strong absorption peak at 3416 cm^{-1}, which can be attributed to the stretching vibration of hydroxyl groups [63] Also N—H stretching bands of the CS amine groups are expected in this region, but these cannot be observed due to the large contribution of the OH stretching vibration, a typical IR pattern for chitosan [63] The absorbance peaks at around 2922 cm^{-1} and 2870 cm^{-1} are attributed to the stretching vibration of C—H bonds. The deformation vibrations of N—H bonds of primary amine appear at 1654 cm^{-1} and 1597 cm^{-1} [64], and the absorption at 1383 cm^{-1} is reflecting the symmetrical deformation vibration of C—H. The FT-IR of PAN shows a typical characteristic absorption peak at 2245 cm^{-1}, which can be attributed by the C≡N stretching vibration [39] The FT-IR spectrum of CS-PAN had the characteristic absorption peaks of both polymers, confirming the deposition of CS on the surface of PAN nanofibers.

The XRD patterns of CS and the CS-PAN composite (Fig. S3). The spectrum of CS exhibits a prominent crystalline peak at $2\theta = 20.12°$, ascribed to diffraction from the (110) crystallographic plane ($d = 4.41$ Å), indicating a highly ordered molecular arrangement. In the XRD spectrum of the CS-PAN composite nanofibers, distinct new diffraction peaks emerge at 17.00° and 29.44° alongside the characteristic CS peak at 20.12° These correspond to PAN's (100) plane ($d = 5.21$ Å) and (101) plane ($d = 3.03$ Å), respectively. Collectively, these observations

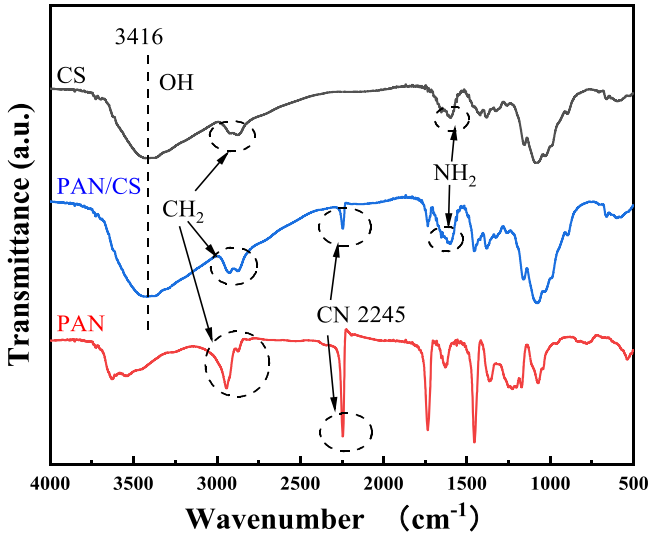

Fig. 6. FT-IR spectra of CS (top, black), CS-PAN composite (middle, blue) and PAN (bottom, red) nanofibers.

confirm that both CS and PAN maintain their structural integrity without significant crystal phase transformation during QCM humidity-sensitive material fabrication. Fig. S4 presents the thermogravimetric (TG) and derivative thermogravimetric (DTG) curves of CS and CS-PAN composite nanofibers under N_2 atmosphere. Both materials exhibit two-stage decomposition behavior: CS shows 77 % total mass loss, while the CS-PAN composite demonstrates 64 % total mass loss. This significant reduction confirms the enhanced thermal stability imparted by PAN nanofibers. In the DTG profiles, the first endothermic peak at 63.5 °C corresponds to desorption of physically adsorbed water. The second endothermic peak at 310.7 °C originates from thermal decomposition of polymer backbones, with covalent bond cleavage and carbonization occurring in the high-temperature region (>400 °C).

3.2. Humidity sensing

To explore the sensing performance of QCM humidity sensors with CS-PAN composite nanofibers as moisture-sensitive coating materials, and to optimize the parameters of QCM humidity sensors, QCM sensors were placed in saturated saline humidity flasks with different relative humidity (the switching time is <2 s). The response of the QCM sensor at different relative humidity is expressed in frequency shifts (Δf). Note that the frequency shift of a QCM sensor exposed to the humidity of 11 % RH caused by LiCl saturated saline solution was selected as the baseline. When the relative humidity of the QCM sensor in the environment is becoming high, the moisture-sensitive material on the surface of the QCM sensor will adsorb more water molecules, and consequently the resonance frequency shift of the QCM sensor will decrease due to the increase of mass loaded.

First, the effect of the deposited mass of the electrospun PAN nanofibers on the on the QCM sensor characteristics was investigated. As explained and shown earlier, the deposited mass of PAN nanofibers on the sensor surface can be controlled by the electrospinning time. When the amount of fiber deposited is too small, it is difficult to construct a 3D network structure on the sensor surface, and the specific surface area of the main moisture-sensitive layer CS cannot be effectively improved. Conversely, large mass loading on the QCM sensor surface results in a reduced sensor resonance signal and an increased layer instability. In this work, the amount of deposited PAN nanofibers is controlled by varying the electrospinning time, and it can be seen from Fig. 7a that as the electrospinning time increases from 30 s to 120 s, the frequency shifts of the QCM sensor at different harmonics ($n = 1$, 5 MHz; $n = 3$, 15 MHz; $n = 5$, 25 MHz) are all decreased, indicating that there are more and more PAN nanofibers deposited on the QCM sensor surface. In more detail, when the electrospinning time is 30 s, 60 s, 90 s, and 120 s, the frequency shift of the QCM sensor at third harmonic ($n = 3$, 15 MHz) can reach −620 Hz, −1138 Hz, −1409 Hz, and −1575 Hz, respectively. After electrospinning the PAN nanofiber modified QCM sensor at different electrospinning times, while maintaining the amount of CS solution, humidity sensing tests were performed of which the QCM data is presented in Fig. 7b Upon increasing the humidity gradually from 11 % RH to 98 % RH, the frequency shifts of all prepared CS-PAN modified QCM sensors at the third harmonic ($n = 3$, 15 MHz) decreased significantly. The frequency responses produced by the four CS-PAN nanofiber modified QCM sensors in each relative humidity environment shows the similar downward trend. However, it can be observed that compared with the other three sensors, the frequency of the CS-PAN nanofiber modified QCM humidity sensor with the PAN electrospinning time of 30

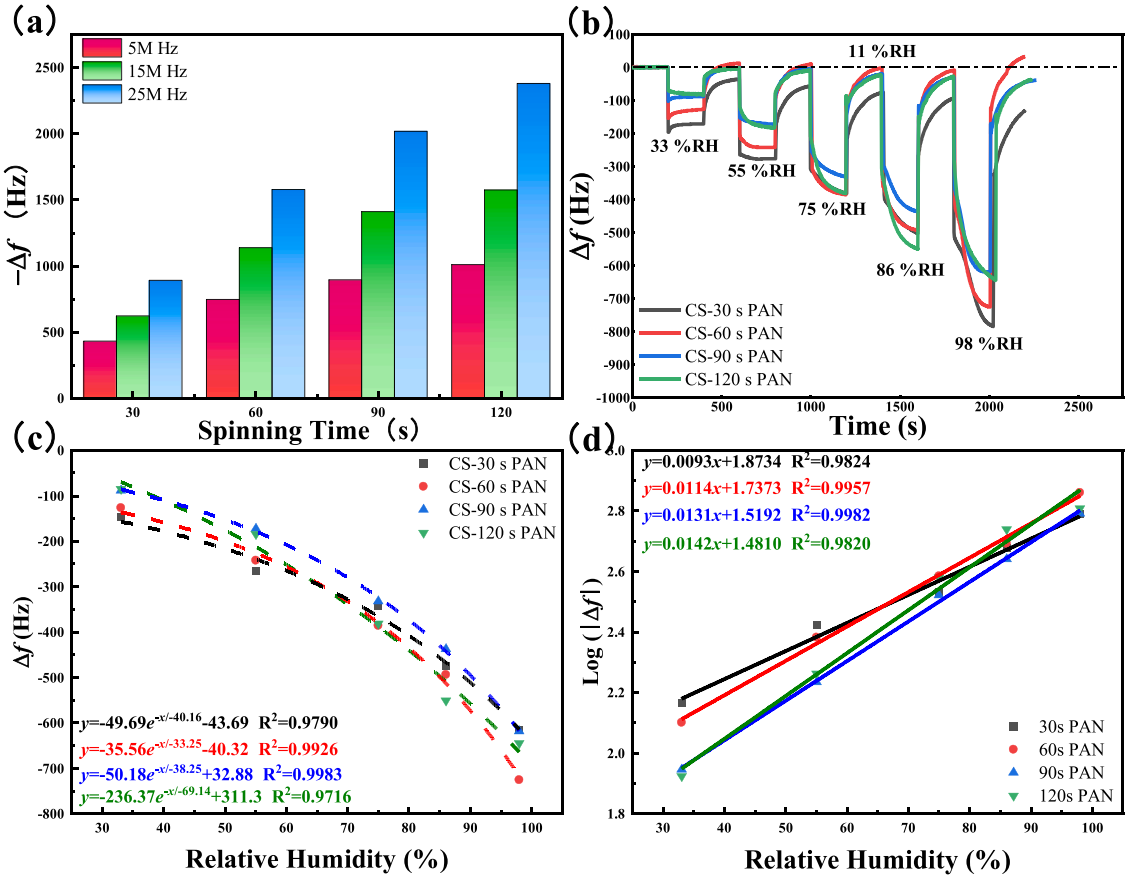

Fig. 7. (**a**) Electrospinning time-dependent frequency responses at different harmonics ($n = 3$, 15 MHz; $n = 5$, 25 MHz; $n = 7$, 35 MHz) of QCM sensors upon PAN nanofiber loading; (**b**) Frequency shift of four CS-PAN nanofiber-modified QCM humidity sensors (obtained at different spinning time) as a function of time at 11–98 % RH; (**c**) Exponential fitting curves of frequency response of four CS-PAN nanofiber modified QCM humidity sensors as a function of 11–98 % RH; (**d**) Logarithmic fitting curves of frequency response of four CS-PAN nanofiber-modified QCM humidity sensors as a function of 11–98 % RH.

s does not fully return to the baseline when the humidity is set to 11 % RH environment. This result may indicate that the amount of PAN nanofiber deposited on the surface of the QCM sensor is too small, and it is difficult to act as a rigid nanoporous network in the CS coating. In addition, CS as a soft and hydrophilic polymer coating has a certain viscoelasticity after exposing it to higher levels of humidity, the oscillation energy of the QCM sensor will be dissipated in the CS coating, leading to energy loss. This may explain why the resonance frequency of the modified QCM sensor does not fully return to the baseline.

The relationship between the frequency response of the QCM sensor and the relative humidity level does not show a linear trend, but rather exhibits an exponential behavior. According to the Brunauer-Emmett-Teller (BET) theory [65], the adsorption capacity of water molecules by QCM sensors is approximately logarithmic at different relative humidities, and water molecules may be adsorbed by multilayer adsorption on CS-PAN composite nanofibers, which is consistent, at least qualitatively, with the test results. Fig. 7c and d show exponential and logarithmic fitting curves of frequency shift of four CS-PAN nanofiber modified QCM humidity sensors as a function of the humidity level ranging from 11 % RH to 98 % RH. The correlation coefficient (R^2) of these fits is above 0.97, which indicates a high correlation between the frequency change and the relative humidity. The unimodal exponential fitting of the frequency changes and the relative humidity has a maximum R^2 value of 0.9983 when the electrospinning time is 90 s, suggesting the best fit within the investigated series. Therefore, for the remaining part of this study, 90 s was chosen as the electrospinning time, while unimodal exponential fittings were performed.

In the composite nanofiber sensing layer, the presence of amino and hydroxyl groups in CS provide sites that allow the binding of water molecules. This makes the amount of CS deposited on the surface of PAN nanofiber a key factor affecting the humidity sensing property of QCM sensors. Upon controlling the spin-coating conditions, including the spin-coating solution volume, the loading amount of CS deposited on the surface of PAN nanofibers can be controlled by varying the concentration of spin-coated CS solution. Fig. 8 shows fitting curves of the frequency response of CS-PAN modified QCM humidity sensor using 0.5 wt. %, 1 wt. %, 1.5 wt. %, 2 wt. %, and 2.5 wt. %

CS under different humidity conditions. From these data is become clear that the frequency shift of the five CS-PAN nanofiber modified QCM sensors generally decreases upon increasing concentration of the CS solution. A high CS concentration, i.e., 2.5 wt. %, leads to a maximum frequency response of 1470 Hz when increasing the humidity from 11 % RH to 98 % RH. This is mainly because the higher the concentration of CS solution: the larger the amount of CS deposited on the surface of PAN nanofibers under the same conditions, the larger the amount of binding sites for water adsorption. The fitting correlation coefficient R^2 of all exponential fittings are >0.92, with a value as high as 0.9998 for the data related to the 2.5 wt. % CS-PAN modified QCM sensor. This result was superior to the previously reported materials that have been used in QCM humidity sensors (Table 2). The sensitivity (S) of a QCM humidity sensor is defined as the ratio of frequency shift to RH change, and in our work S is up to 16.9 Hz/ % RH. In addition, the limit of detection (LOD) value of our QCM humidity sensor is calculated to be 0.089 % RH. LOD points to the lowest RH change that can be detected with the developed device. Furthermore our study shows that if the concentration of the coated CS solution is further increased, the vibration of the QCM sensor is unstable or even stop vibrating.

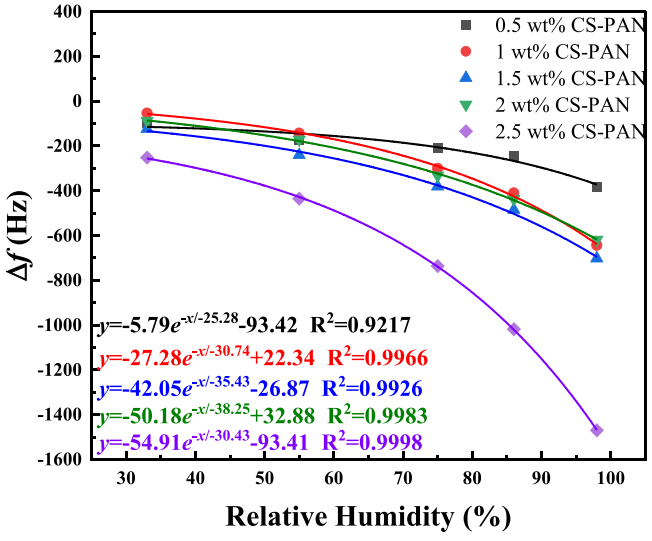

Fig. 8. Fitting curves of the frequency response of CS-PAN modified QCM humidity sensor using 0.5 wt. %, 1 wt. %, 1.5 wt. %, 2 wt. %, and 2.5 wt. % CS under different humidity conditions.

To conclude this part of our work, for an electrospinning time of 90 s, a CS-PAN modified QCM sensor with a CS concentration of 2.5 wt. % gives the best results in term of the fitting. Humidity sensing validation experiments confirmed that this optimized fiber architecture and mass loading effectively enhance the moisture response sensitivity of chitosan coatings, meeting requirements for high-precision humidity sensing applications.

Next, Fig. 9a shows the frequency response curve of a CS-PAN nanofiber modified QCM humidity sensor in the range of 11 % RH to 98 % RH. It can be seen that the change in the resonance frequency increases with the relative humidity, indicating more adsorption of water molecules by the CS-PAN moisture-sensitive layer on the surface of the QCM sensor. When the humidity to which the CS-PAN nanofiber modified QCM sensor is exposed is set to the low humidity level again (i. e. 11 % RH) the signal returns to the baseline. This full reversibility indicates that the water molecules adsorbed by the moisture sensitive layer are gradually desorbed. Fig. 9b shows frequency variations (Δf) and mass changes (Δm) calculated using Eq. (1) for different humidity values (33–98 % RH).

Response time and recovery time are important indicators to evaluate the practicality of humidity sensors and are usually reported to reflect the response characteristics of the sensor [39] The response time during adsorption or the recovery time during desorption is usually defined as the time needed to reach 90 % of the full frequency shift of the QCM humidity sensor [64] Fig. 9c and d show the response-recovery time of the CS-PAN nanofiber modified QCM humidity sensor at the low and high humidity level. It can be seen that the response-recovery time of the CS-PAN nanofiber modified sensors in low humidity environment (11–33 % RH) and high humidity environment (11–98 % RH) is <4 s/33.4 s and 21 s/63 s, respectively. This significant difference may be related to different mechanisms of water adsorption by the CS-PAN

Table 2
Selected data from reported QCM humidity sensor studies, including the results of our work.

Materials	Measurement range (% R-H)	Frequency shift (Hz)	Correlation coefficient(R^2)	Ref.
PAN-PEI	33–75	−7112	0.994	[39]
PVA/nano-silica	11.31–85.11	<−1800	0.9990	[43]
Bacterial cellulose	5–97	−1306	0.9980	[66]
PDMAEM-PGMA	20–97	–	0.9860	[67]
PEI-PA6	2–95	−1678	0.9988	[68]
PVA-ZnO	10–90	−43	0.9966	[69]
$Cu(OH)_2$	11–84	−6269	0.994	[70]
$Cu(OH)_2$-GO	0–80	−4170	0.9968	[71]
PPy	0–97	−2025	0.9973	[3]
PPy-CS	0–97	−5132	0.9975	[3]
CS-PAN	**11–98**	**−1470**	**0.9998**	This work

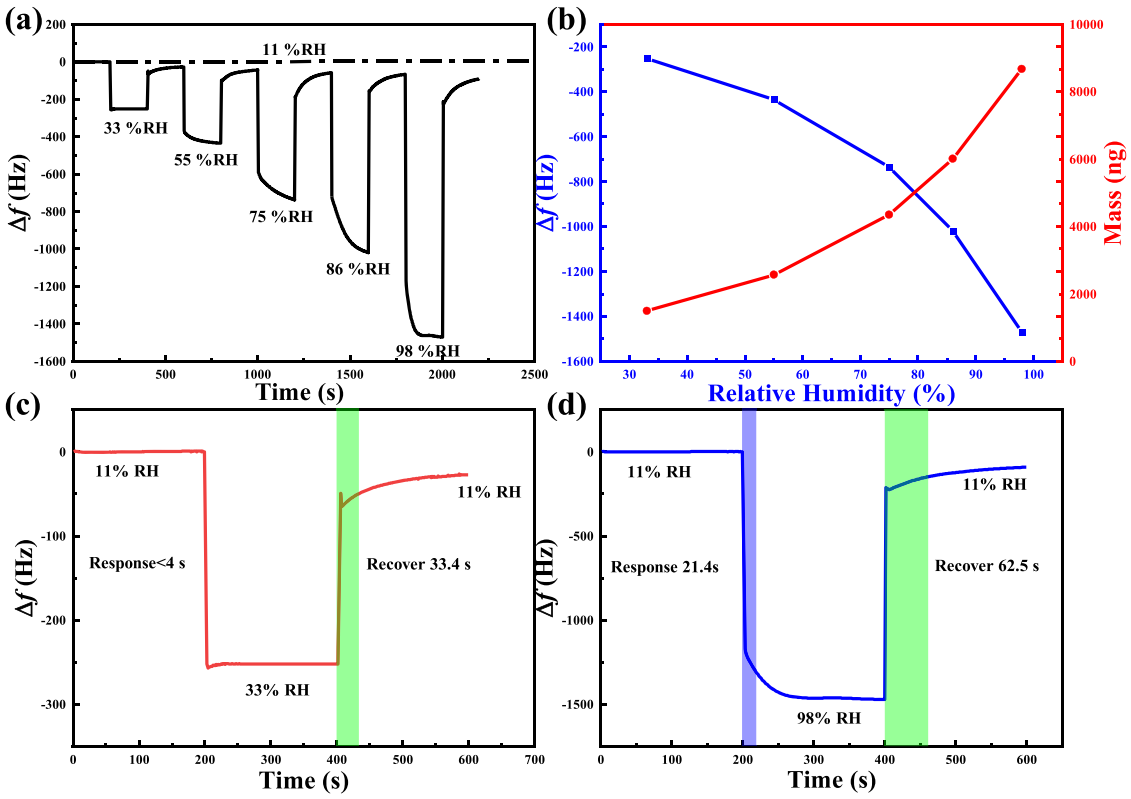

Fig. 9. QCM data of a CS-PAN composite nanofiber under various humidity conditions: (**a**) Dynamic frequency response curve at 11–98 % RH; (**b**) Frequency variation (Δ*f*) and mass change (Δ*m*) at different humidity; (**c**) Response-recovery time at low humidity (11–33 % RH); (**d**) Response-recovery time at high humidity (11–98 % RH).

nanofiber moisture-sensitive materials at low humidity and high humidity environments (vide infra). This would also explain the non-linear relationship between frequency shift and relative humidity level. Nevertheless, the CS-PAN nanofiber modified QCM humidity sensor has a response-recovery time at different humidity environments as short as 4 s/33.4 s.

The introduction of PAN nanofibers is not only aimed to increase the deposited amount of CS chains after spinning coating on the QCM sensor, increase the specific surface area of CS coating, and provide more adsorption sites for water molecules, but also to provide increased rigidity of the CS coating.

Fig. 10a presents the dynamic frequency response curves of a pure (i.e., 100 %, so PAN-free) CS-coated and CS-PAN coated QCM humidity sensor over 11–98 % RH. From Fig. 10a, it can be seen that the CS-coated QCM sensor also responds to the relative humidity, but its frequency change in the range of 11 % RH to 98 % RH is significantly smaller than that of the CS-PAN nanofiber modified QCM humidity sensor (488 vs. 1470 Hz at 98 % RH). Next to mechanical stabilization, the use of PAN nanofibers results in a threefold increase in sensitivity, which can be attribute to synergistic interfacial effects. In addition, compared with the CS-PAN nanofiber modified QCM sensor, the frequency signal of the CS-coated QCM humidity sensor returns to the baseline when changing from the high humidity environment to the low humidity environment. Also, at high humidity, the desorption time of water molecules significantly increased, and the resonance frequency of QCM sensor does not fully return to the initial state. These differences can be understood by the nature of CS, as it is a natural, hydrophilic polymer with a high density of amino and hydroxyl groups, which can interact with – and absorb – water molecules, making it easy to hydrate when exposed to elevated humidity.

The increasing viscoelasticity of CS with increasing humidity results in the dissipation of the energy related to the oscillation of the QCM sensor, thus leading to a difference in the resonance frequency of QCM sensor at different humidity. When PAN nanofibers are introduced in the moisture-sensitive CS layer to support the rigidity of the coating, resulting in an increased coating stability, the effect of humidity on the sensing is less pronounced. Fig. 10b, c, and d show the humidity-dependent frequency response curves of pure CS and CS-PAN nanofiber modified QCM sensors and the humidity hysteresis curves for pure CS-coated and CS-PAN composite nanofiber modified QCM sensors, respectively. Fig. 10b shows, for both samples, a comparable trend than the data presented in Fig. 10a upon increasing humidity, albeit with a slightly lower sensitivity effect due to PAN (1549.7 vs. 583.3 Hz at 98 % RH, that is a factor of 2.66). Cycling back to a low humidity gives insight in the hysteresis of the response. In more detail, this parameter refers to the non-coincidence of the response curves of the sensor in the process of the adsorption and desorption of water at different humidity levels. It can be obtained by calculation the ratio of the maximum difference in the adsorption and desorption response curves compared to the full scale frequency change [41] The maximum hysteresis error (H_e) of both QCM humidity sensors is observed around 75 % RH. The introduction of PAN nanofibers into the CS moisture-sensitive layer, results in a decrease of the maximum hysteresis error decreases (from ~13 % RH to 9 % RH), a reflection of the improved stability of the sensor coating.

Fig. 11a shows the QCM data of short-term (multiple hours) and long-term (multiple weeks) repeatability experiment of the CS-PAN nanofiber modified QCM humidity sensor. From Fig. 11a, it can be seen that with an average frequency of 1431±31 Hz and a gradually decrease from 1475 to 1407 Hz, the CS-PAN nanofiber modified QCM humidity sensor shows a good repeatability over five consecutive changes from 11 to 98 % RH. The stability of the CS-PAN nanofiber modified QCM humidity sensors exposed in 33 % RH, 55 % RH, 75 % RH, 86 % RH, and 98 % RH environments was tested over 15 days, and it can be seen from Fig. 11b that the difference in the frequency response

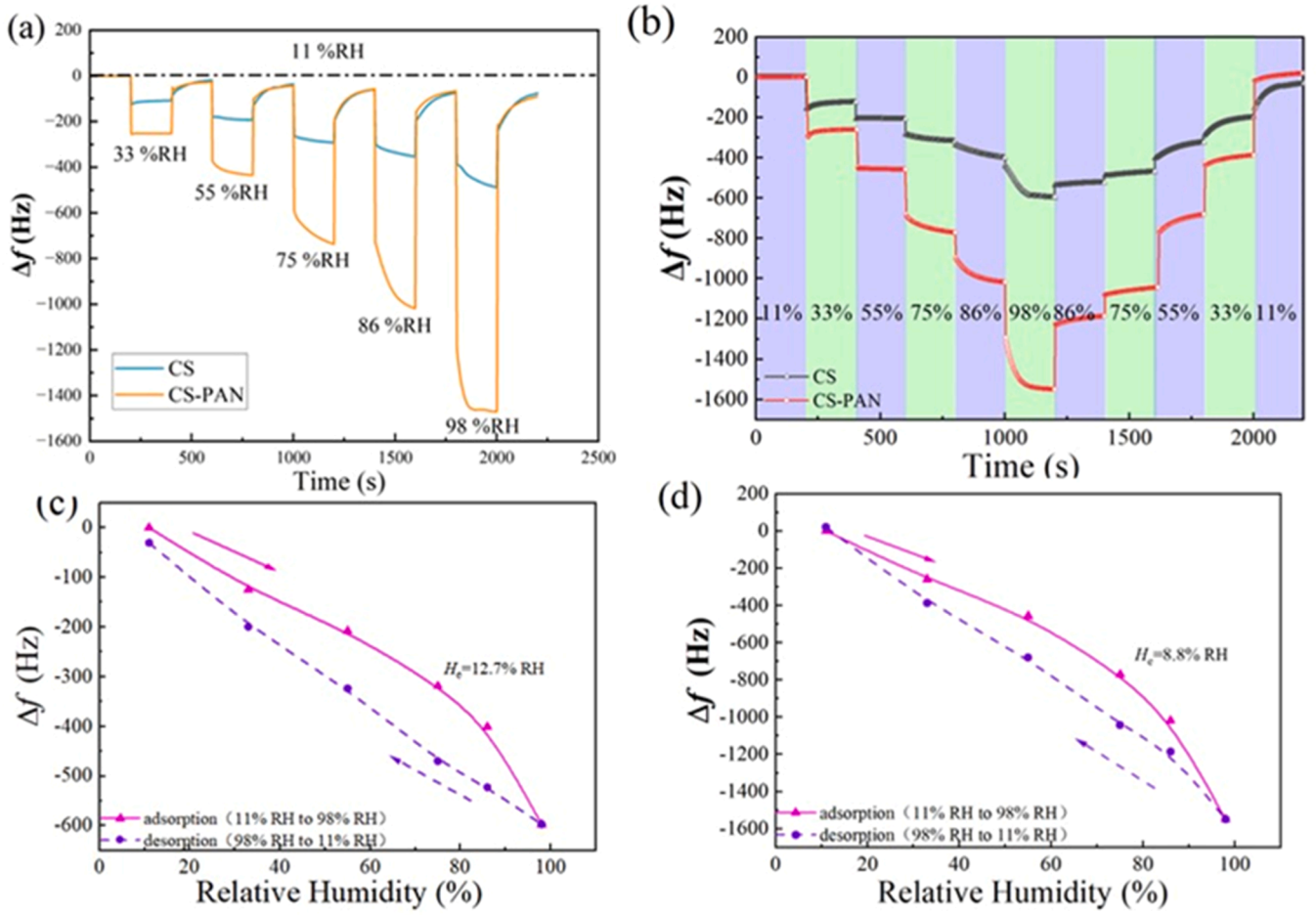

Fig. 10. (**a**) Dynamic frequency response curve of pure CS-coated (blue) and CS-PAN-coated (orange) QCM humidity sensor at 11–98 % RH; (**b**) Response curves of pure CS (black) and CS-PAN (red) nanofiber modified QCM sensors from low humidity to high humidity to low humidity; (**c**) Humidity hysteresis curves for pure CS-coated QCM sensor and (**d**) CS-PAN composite nanofiber modified QCM sensor.

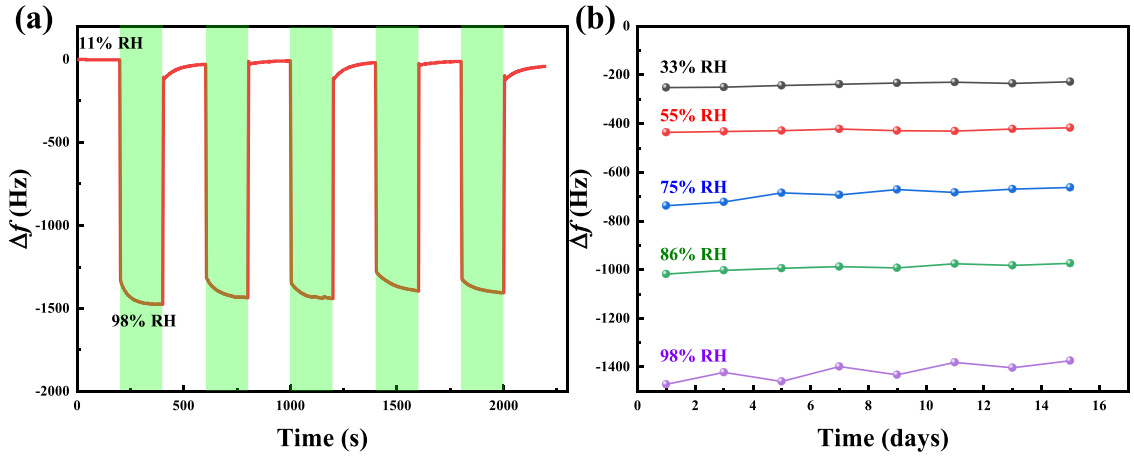

Fig. 11. CS-PAN nanofiber modified QCM humidity sensor: (**a**) short-term repeatability; (**b**) Long-term repeatability.

of the sensors is within 2.45 %.

Next, a comparative analysis of ΔΓ variations between CS-functionalized and CS-PAN-functionalized QCM sensors over 11–98 % RH was performed (Fig. 12a). Usually, ΔΓ is used to characterize the viscoelastic performance of a thin layer or film on QCM sensors [25] The presence of a rigid, thin layer results in a small ΔΓ value, possibly close to 0, while a soft, wet, and hydrated layer results in higher ΔΓ, up to a few dozens [20,30] When the CS-PAN nanofiber layer is loaded on the surface of QCM sensor, the resonance frequency of the sensor decreases due to the increase in mass, as explained earlier, and the ΔΓ becomes larger accordingly, pointing to a hydrated, soft film.

From Fig. 12a, it can be observed that the ΔΓ values of both QCM humidity sensors increase upon increasing the humidity level. This is the result of an increased energy loss due to higher levels of water

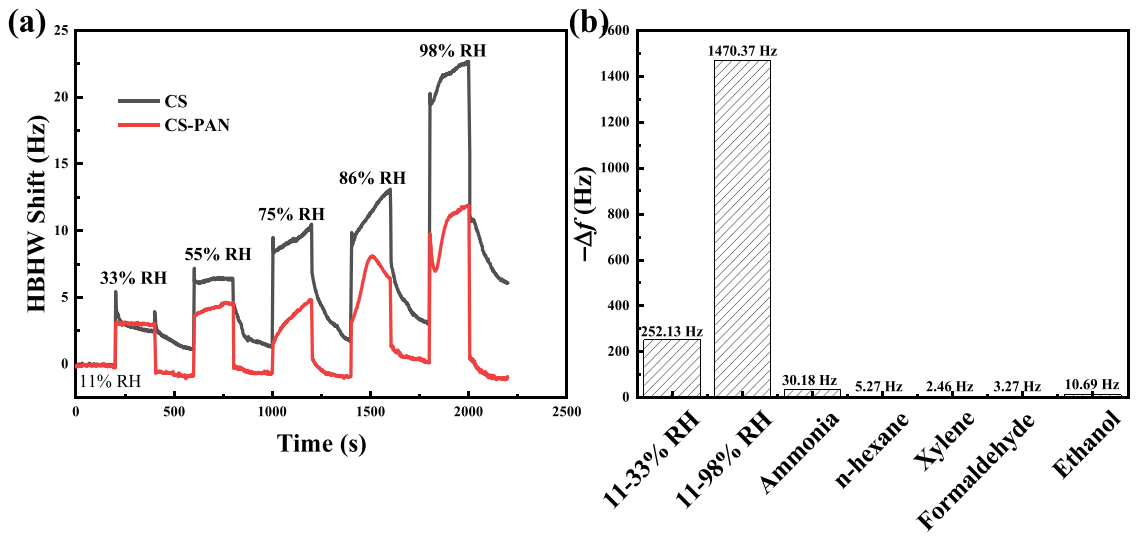

Fig. 12. (**a**) Half-band-half-width shift (ΔΓ) of CS and CS-PAN modified QCM humidity sensors exposed in different humidity environment and (**b**) Frequency responses of CS-PAN nanofiber modified QCM humidity sensor to various gases.

adsorption and – consequently – increased viscoelasticity of the moisture sensitive layer. In more detail, the ΔΓ value for the pure CS-coated QCM sensor increased by 22.7 Hz upon increasing the humidity from 11 % to 98 % RH. In contrast, the CS-PAN composite-coated sensor exhibited a significantly smaller ΔΓ increase of only 11.9 Hz, representing a reduction by almost a factor of two compared to pure CS. The observed ΔΓ changes indicate that water molecules interact with amino groups in CS through hydrogen bonding, causing structural rearrangements and increased viscoelastic dissipation as the sensing coating hydrates. Upon the introduction of PAN nanofibers as the supporting framework of CS, ΔΓ decreased, proving that the stability of CS-PAN nanofiber modified QCM humidity sensor in high humidity environment has been improved. The attenuated ΔΓ rise in the CS-PAN modified sensor confirms that PAN nanofibers provide mechanical stabilization, thereby suppressing humidity-induced softening of the chitosan matrix.

Fig. 12b shows the results of the selectivity testing of this CS-PAN nanofiber modified QCM humidity sensor in 33 % RH, 98 % RH, and five common volatile organic compounds (VOCs, here ammonia, n-hexane, xylene, formaldehyde, and ethanol). Compared to water, the results show low QCM responses to other gases, indicating a high selectivity and suitability for humidity sensing. Note that the concentration of VOCs was controlled by adding a 10 μL of liquid into a container with a fixed volume of 3.375 L, and QCM tests were then performed after the organic gas volatilization was allowed to reach equilibrium in 30 mins.

3.3. Sensing mechanism of CS-PAN modified QCM sensor

The QCM results show that, compared with pure CS-coated QCM sensor, CS-PAN composite nanofiber modified QCM humidity sensor has better humidity sensing characteristics. On the one hand, CS contains a large number of hydrophilic functional groups, including amino and hydroxyl groups, which can provide a large number of adsorption active sites for adsorbing water molecules by forming hydrogen bonds. On the other hand, PAN nanofibers can act as a supporting framework in CS, which not only has a porous structure, which increases the surface area of CS, but also provides a certain rigid structure for the natural polymer CS, reducing the energy loss caused by viscoelasticity during the sensor oscillation, and improving the sensing stability of the moisture-sensitive layer. In addition, the porous network structure of PAN nanofibers loaded on the surface of QCM sensor allows more adsorption of CS chains onto the PAN nanofibers. The water adsorption site can be further improved. In the synergy of many aspects, it plays an important role in ensuring the moisture sensitivity characteristics of the CS-PAN modified QCM humidity sensor.

The humidity sensing of prepared QCM sensors mainly relies on the interaction of water molecules with the amino groups and hydroxyl groups on the CS surface. Water molecules can form hydrogen bonds with these hydrophilic groups. Fig. 13 shows a schematic of the CS-PAN composite nanofibers onto which water molecules are adsorbed under two different humidity environments: low (left) and high (right) humidity. In a low humidity environment, the number of water molecules is small, and the number of available adsorption sites on the moisture-sensitive CS-PAN layer is relatively sufficient. Under these conditions, the water molecules are adsorbed, the hydrogen bonds are formed, and the equilibrium is reached quickly. In a high humidity environment, excess water molecules will combine with the first adsorbed water molecules in the form of hydrogen bonds, and more water molecules will enter the humidity-sensitive layer, resulting in the swelling of the humidity-sensitive layer, further affecting the frequency shift and significantly increasing the response time of QCM sensors.

4. Conclusions and outlook

A QCM humidity sensor based on CS-PAN composite nanofibers was prepared successfully by compounding functional and hydrophilic CS with electrospun PAN nanofibers using a simple spin-coating method. The combination of a 2.5 wt. % CS solution and a deposition time of PAN nanofibers of 90 s resulted in a CS-PAN nanofiber modified QCM humidity sensor showing optimal sensing characteristics with a high fitting coefficient (R^2=0.9998), high sensitivity (16.9 Hz/ % RH), low humidity

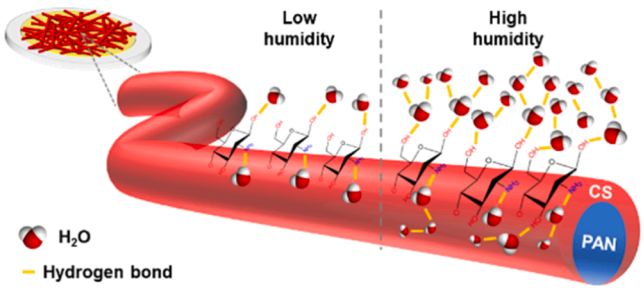

Fig. 13. Scheme illustrating the adsorption of water molecules onto CS-PAN composite nanofibers under two different humidity environments: low (left) and high (right) humidity.

hysteresis (8.8 % RH), and short response recovery time (at low humidity < 4 s/33 s, at high humidity 21 s/63 s), good repeatability, stability, and high selectivity. The frequency changes increased upon increasing amounts of CS, which can be understood by the increased number of sites that are able to interacted with water. The addition of PAN does not only result in increased accessibility of these sites, it also proved to contribute to the stability of the coating.

To conclude, this composite sensor concept, based on electrospinning polymer fibers following by spin-coating a hydrophilic biopolymer, has the potential to be used for the intelligent detection of real-time humidity at room temperature and/or the diagnosis of medical and respiratory monitoring. More generally, the further development of gas sensors is expected to benefit from technological advancements in the field of learning-based strategies focusing on sensor performance [72] and the required characteristics of (bio)nanomaterials [73], which is also relevant for affinity coating innovations in a broader field [74], including self-powered [75], flexible [76], and wearable sensors [77]

CRediT authorship contribution statement

Jialin Liu: Writing – original draft, Validation, Software, Methodology, Investigation, Formal analysis, Data curation. **Yuxuan Zhang:** Methodology, Investigation. **Wang Qin:** Methodology, Funding acquisition. **Xiaowang Lu:** Data curation. **Yanhua Cai:** Software, Investigation. **Junfeng Cheng:** Formal analysis. **Chunlin Liu:** Conceptualization. **Louis C.P.M. de Smet:** Writing – review & editing, Visualization, Formal analysis. **Zheng Cao:** Writing – review & editing, Validation, Supervision, Resources, Project administration, Funding acquisition.

Declaration of competing interest

The authors declare that they have no known competing financial interests or personal relationships that could have appeared to influence the work reported in this paper.

Acknowledgements

This project is supported by the National Natural Science Foundation of China (Grant No. 21704008, 21644002). Further financial support for this project provided by the Priority Academic Program Development of Jiangsu Higher Education Institutions (PAPD), the Top-notch Academic Programs Project of Jiangsu Higher Education Institutions (TAPP), and the Postgraduate Research & Practice Innovation Program of Jiangsu Province is also gratefully acknowledged (SJCX22_1329). L.C.P.M.d.S is supported by the Dutch Research Council (NWO START-UP Grant 740.018.004).

Supplementary materials

Supplementary material associated with this article can be found, in the online version, at doi:10.1016/j.surfin.2025.107302.

Data availability

Data will be made available on request.

References

[1] X. Li, Z. Zhuang, D. Qi, C. Zhao, High sensitive and fast response humidity sensor based on polymer composite nanofibers for breath monitoring and non-contact sensing, Sens. Actuators, B 330 (2021) 129239, https://doi.org/10.1016/j.snb.2020.129239.

[2] F. Fauzi, A. Rianjanu, I. Santoso, K. Triyana, Gas and humidity sensing with quartz crystal microbalance (QCM) coated with graphene-based materials – A mini review, Sens. Actuators, B 330 (2021) 112837, https://doi.org/10.1016/j.sna.2021.112837.

[3] X. Liu, D. Zhang, D. Wang, T. Li, X. Song, Z. Kang, A humidity sensing and respiratory monitoring system constructed from quartz crystal microbalance sensors based on a chitosan/polypyrrole composite film, J. Mater. Chem. A 9 (25) (2021) 14524–14533, https://doi.org/10.1039/D1TA02828F, 10.1039/D1TA02828F.

[4] D.-L. Wen, Y.-X. Pang, P. Huang, Y.-L. Wang, X.-R. Zhang, H.-T. Deng, X.-S. Zhang, Silk Fibroin-Based Wearable All-Fiber Multifunctional Sensor for Smart Clothing, Adv. Fiber Mater. 4 (4) (2022) 873–884, https://doi.org/10.1007/s42765-022-00150-x.

[5] M. Sajid, Z.J. Khattak, K. Rahman, G. Hassan, K.H. Choi, Progress and future of relative humidity sensors: a review from materials perspective, Bull. Mater. Sci. 45 (4) (2022) 238, https://doi.org/10.1007/s12034-022-02799-x.

[6] P.-G. Su, C.-L. Uen, A resistive-type humidity sensor using composite films prepared from poly(2-acrylamido-2-methylpropane sulfonate) and dispersed organic silicon sol, Talanta 66 (5) (2005) 1247–1253, https://doi.org/10.1016/j.talanta.2005.01.039.

[7] R. Zhou, J. Li, H. Jiang, H. Li, Y. Wang, D. Briand, M. Camara, G. Zhou, N.F. de Rooij, Highly transparent humidity sensor with thin cellulose acetate butyrate and hydrophobic AF1600X vapor permeating layers fabricated by screen printing, Sens. Actuators, B 281 (2019) 212–220, https://doi.org/10.1016/j.snb.2018.10.061.

[8] R. Najjar, S. Nematdoust, A resistive-type humidity sensor based on polypyrrole and ZnO nanoparticles: hybrid polymers vis-a-vis nanocomposites, RSC. Adv. 6 (113) (2016) 112129–112139, https://doi.org/10.1039/C6RA24002J, 10.1039/C6RA24002J.

[9] Y. Chen, R. Xie, B. Zou, Y. Liu, K. Zhang, S. Li, B. Zheng, W. Zhang, J. Wu, F. Huo, CNT@leather-based electronic bidirectional pressure sensor, Sci. China Technol. Sci. 63 (10) (2020) 2137–2146, https://doi.org/10.1007/s11431-019-1502-7.

[10] M.A. Najeeb, Z. Ahmad, R.A. Shakoor, Organic Thin-Film Capacitive and Resistive Humidity Sensors: a Focus Review, Adv. Mater. Interfaces 5 (21) (2018) 1800969, https://doi.org/10.1002/admi.201800969.

[11] S. Atalay, S. Erdemoğlu, V.S. Kolat, T. İzgi, E. Akgeyik, H.C. Yılmaz, H. Kaya, F. E. Atalay, A rapid response humidity sensor for monitoring human respiration with TiO2-based nanotubes as a sensing layer, J. Electron. Mater. 49 (5) (2020) 3209–3215, https://doi.org/10.1007/s11664-020-08006-z.

[12] K.S. Schanze, Forum on materials and interfaces for next-generation thin-film transistors, ACS Appl. Mater. Interfaces 10 (31) (2018) 25833, https://doi.org/10.1021/acsami.8b12147. -25833.

[13] R. Gupta, J. Luan, S. Chakrabartty, E.L. Scheller, J. Morrissey, S. Singamaneni, Refreshable nanobiosensor based on organosilica encapsulation of biorecognition elements, ACS Appl. Mater. Interfaces 12 (5) (2020) 5420–5428, https://doi.org/10.1021/acsami.9b17506.

[14] R. Schirhagl, Bioapplications for molecularly imprinted polymers, Anal. Chem. 86 (1) (2014) 250–261, https://doi.org/10.1021/ac401251j.

[15] B. García-Farrera, L.F. Velásquez-García, Ultrathin Ceramic piezoelectric films via room-temperature electrospray deposition of ZnO nanoparticles for Printed GHz devices, ACS Appl. Mater. Interfaces 11 (32) (2019) 29167–29176, https://doi.org/10.1021/acsami.9b09563.

[16] D. Barauskas, S.J. Park, D. Pelenis, G. Vanagas, J.J. Lee, D. Viržonis, C.W. Jones, J. Baltrusaitis, CO2 and SO2 Interactions with Methylated Poly(ethylenimine)-functionalized capacitive micromachined ultrasonic transducers (CMUTs): gas sensing and degradation mechanism, ACS Appl. Electron. Mater. 1 (7) (2019) 1150–1161, https://doi.org/10.1021/acsaelm.9b00151.

[17] J.H. Park, S.G. Song, M.H. Shin, C. Song, H.Y. Bae, N-Triflyl phosphoric triamide: a high-performance purely organic trifurcate quartz crystal microbalance sensor for chemical warfare agent, ACS. Sens. 7 (2) (2022) 423–429, https://doi.org/10.1021/acssensors.1c02715.

[18] Y. Yao, X.-h. Huang, B.-y. Zhang, Z. Zhang, D. Hou, Z.-k. Zhou, Facile fabrication of high sensitivity cellulose nanocrystals based QCM humidity sensors with asymmetric electrode structure, Sens. Actuators, B 302 (2020) 127192, https://doi.org/10.1016/j.snb.2019.127192.

[19] J. Song, X. Lin, L.Y. Ee, S.F.Y. Li, M. Huang, A Review on electrospinning as versatile supports for diverse nanofibers and their applications in environmental sensing, Adv. Fiber Mater. (2022), https://doi.org/10.1007/s42765-42022-00237-42765, 10.1007/s42765-022-00237-5.

[20] Z. Cao, Y. Chen, Q. Zhang, Y. Xia, G. Liu, D. Wu, W. Ma, J. Cheng, C. Liu, Preparation and ion sensing property of the self-assembled microgels by QCM, Nanofabrication. 3 (1) (2017) 16–25, https://doi.org/10.2478/nanofab-2017-0002 (acccessed 2022-11-10).

[21] Z. Cao, B. Du, T. Chen, H. Li, J. Xu, Z. Fan, Fabrication and properties of thermosensitive organic/inorganic Hybrid Hydrogel Thin Films, Langmuir. 24 (10) (2008) 5543–5551, https://doi.org/10.1021/la8000653.

[22] Z. Cao, P.I. Gordiichuk, K. Loos, E.J.R. Sudhölter, L.C.P.M. de Smet, The effect of guanidinium functionalization on the structural properties and anion affinity of polyelectrolyte multilayers, Soft. Matter. 12 (5) (2016) 1496–1505, https://doi.org/10.1039/C5SM01655J, 10.1039/C5SM01655J.

[23] Z. Cao, J. Guo, X. Fan, J. Xu, Z. Fan, B. Du, Detection of heavy metal ions in aqueous solution by P(MBTVBC-co-VIM)-coated QCM sensor, Sens. Actuators, B 157 (1) (2011) 34–41, https://doi.org/10.1016/j.snb.2011.03.023.

[24] Z. Cao, T. Tsoufis, T. Svaldo-Lanero, A.-S. Duwez, P. Rudolf, K. Loos, The Dynamics of Complex Formation between Amylose Brushes on Gold and Fatty Acids by QCM-D, Biomacromolecules. 14 (10) (2013) 3713–3722, https://doi.org/10.1021/bm4010904.

[25] Z. Cao, Y. Zhang, Z. Luo, W. Li, T. Fu, W. Qiu, Z. Lai, J. Cheng, H. Yang, W. Ma, et al., Construction of a Self-Assembled Polyelectrolyte/Graphene Oxide Multilayer Film and Its Interaction with Metal Ions, Langmuir. 37 (41) (2021) 12148–12162, https://doi.org/10.1021/acs.langmuir.1c02058.

[26] J. He, Y. Wu, J. Wu, X. Mao, L. Fu, T. Qian, J. Fang, C. Xiong, J. Xie, H. Ma, Study and application of a linear frequency–thickness relation for surface-initiated atom

transfer radical polymerization in a quartz crystal microbalance, Macromolecules. 40 (9) (2007) 3090–3096, https://doi.org/10.1021/ma062613n.
[27] C. Ma, H. Zhou, B. Wu, G. Zhang, Preparation of Polyurethane with zwitterionic side chains and their protein resistance, ACS Appl. Mater. Interfaces 3 (2) (2011) 455–461, https://doi.org/10.1021/am101039q.
[28] K. Triyana, A. Sembiring, A. Rianjanu, S.N. Hidayat, R. Riowirawan, T. Julian, A. Kusumaatmaja, I. Santoso, R. Roto, Chitosan-based quartz crystal microbalance for alcohol sensing, Electronics. (Basel) 7 (9) (2018), https://doi.org/10.3390/electronics7090181.
[29] L. Wang, Metal-organic frameworks for QCM-based gas sensors: a review, Sens. Actuators, A (2020) 307. From Cnki.
[30] Y. Wu, Y. Zhang, K. Wang, Z. Luo, Z. Xue, H. Gao, Z. Cao, J. Cheng, C. Liu, L. Zhang, Construction of self-assembled polyelectrolyte/cationic microgel multilayers and their interaction with anionic dyes using quartz crystal microbalance and atomic force microscopy, ACS. Omega 6 (8) (2021) 5764–5774, https://doi.org/10.1021/acsomega.0c06181.
[31] G. Zhang, Study on Conformation Change of Thermally Sensitive Linear Grafted Poly(N-isopropylacrylamide) Chains by Quartz Crystal Microbalance, Macromolecules. 37 (17) (2004) 6553–6557, https://doi.org/10.1021/ma035937+.
[32] J. Zhang, S. Xu, H. Jin, G. Liu, Ionic hydrogen bond effects on polyelectrolyte brushes beyond the hydronium and hydroxide ions, Chem. Commun. 56 (74) (2020) 10930–10933, https://doi.org/10.1039/D0CC03763J, 10.1039/D0CC03763J.
[33] T.A. Blank, L.P. Eksperiandova, K.N. Belikov, Recent trends of ceramic humidity sensors development: a review, Sens. Actuators, B 228 (2016) 416–442, https://doi.org/10.1016/j.snb.2016.01.015.
[34] K.-S. Chou, C.-H. Lee, B.-T. Liu, Effect of Microstructure of ZnO nanorod film on humidity sensing, J. Am. Ceram. Soc. 99 (2) (2016) 531–535, https://doi.org/10.1111/jace.13994, 10.1111/jace.13994 (acccessed 2022/03/07).
[35] M. Zhang, C. Han, W.-Q. Cao, M.-S. Cao, H.-J. Yang, J. Yuan, A nano-micro engineering nanofiber for electromagnetic absorber, green shielding and sensor, Nano-Micro Letters 13 (1) (2020) 27, https://doi.org/10.1007/s40820-020-00552-9.
[36] J. Cai, C. Lv, E. Aoyagi, S. Ogawa, A. Watanabe, Laser direct writing of a high-performance all-graphene humidity sensor working in a novel sensing mode for portable electronics, ACS Appl. Mater. Interfaces 10 (28) (2018) 23987–23996, https://doi.org/10.1021/acsami.8b07373.
[37] L. Ji, Y. Pan, Z. Cao, R. Wang, H. Yang, J. Cheng, C. Liu, X. Lu, L.C.P.M de Smet, Facile preparation of graphene oxide/Poly (-Isopropylacrylamide–acrylic acid) composite thin film and its quartz crystal microbalance humidity sensing property, J. Polymer Sci. 62 (23) (2024) 5398–5410, https://doi.org/10.1002/pol.20240504 (acccessed 2025/03/19).
[38] Y. Li, M. Jiao, H. Zhao, M. Yang, Humidity sensing properties of the composite of electrospun crosslinked polyelectrolyte nanofibers decorated with Ag nanoparticles, Sens. Actuators, B 273 (2018) 133–142, https://doi.org/10.1016/j.snb.2018.06.009.
[39] A. Rianjanu, T. Julian, S.N. Hidayat, N. Yulianto, N. Majid, I. Syamsu, H.S. Wasisto, K. Triyana, Quartz crystal microbalance humidity sensors integrated with hydrophilic polyethyleneimine-grafted polyacrylonitrile nanofibers, Sens. Actuators, B 319 (2020) 128286, https://doi.org/10.1016/j.snb.2020.128286.
[40] S.K. Vashist, P. Vashist, Recent advances in quartz crystal microbalance-based sensors, J. Sens. 2011 (2011) 571405, https://doi.org/10.1155/2011/571405.
[41] J. Yang, L. Feng, Y. Chen, L. Feng, J. Lu, L. Du, J. Guo, Z. Cheng, Z. Shi, L. Zhao, High-sensitivity and environmentally friendly humidity sensors deposited with recyclable green microspheres for wireless monitoring, ACS Appl. Mater. Interfaces 14 (13) (2022) 15608–15622, https://doi.org/10.1021/acsami.2c00489.
[42] Z. Yuan, H. Tai, Z. Ye, C. Liu, G. Xie, X. Du, Y. Jiang, Novel highly sensitive QCM humidity sensor with low hysteresis based on graphene oxide (GO)/poly (ethyleneimine) layered film, Sens. Actuators, B 234 (2016) 145–154, https://doi.org/10.1016/j.snb.2016.04.070.
[43] X. Zheng, R. Fan, C. Li, X. Yang, H. Li, J. Lin, X. Zhou, R. Lv, A fast-response and highly linear humidity sensor based on quartz crystal microbalance, Sens. Actuators, B 283 (2019) 659–665, https://doi.org/10.1016/j.snb.2018.12.081.
[44] Y. Wu, T. Fu, H. Gao, Z. Cao, J. Cheng, C. Liu, G. Tao, D. Wu, Preparation and moisture absorption behavior of PAM/CS/GO hydrogels, J. Funct. Polym. 34 (04) (2021) 394–400, https://doi.org/10.14133/j.cnki.1008-9357.20201221001. From Cnki.
[45] M. Tang, X. Liu, D. Zhang, H. Zhang, G. Xi, Ultra-sensitive humidity QCM sensor based on sodium alginate/polyacrylonitrile composite film for contactless Morse code communication, Sensors Actuators B: Chem. 407 (2024) 135429, https://doi.org/10.1016/j.snb.2024.135429.
[46] J. Nie, W. Lu, J. Ma, L. Yang, Z. Wang, A. Qin, Q. Hu, Orientation in multi-layer chitosan hydrogel: morphology, mechanism and design principle, Sci. Rep. 5 (1) (2015) 7635, https://doi.org/10.1038/srep07635.
[47] P.T. Sudheesh Kumar, V.-K. Lakshmanan, T.V. Anilkumar, C. Ramya, P. Reshmi, A. G. Unnikrishnan, S.V. Nair, R. Jayakumar, Flexible and microporous chitosan Hydrogel/Nano ZnO composite bandages for wound dressing: in vitro and in vivo evaluation, ACS Appl. Mater. Interfaces 4 (5) (2012) 2618–2629, https://doi.org/10.1021/am300292v.
[48] C. Zhang, Y. Dai, Y. Wu, G. Lu, Z. Cao, J. Cheng, K. Wang, H. Yang, Y. Xia, X. Wen, et al., Facile preparation of polyacrylamide/chitosan/Fe3O4 composite hydrogels for effective removal of methylene blue from aqueous solution, Carbohydr. Polym. 234 (2020) 115882, https://doi.org/10.1016/j.carbpol.2020.115882.
[49] Z. Ahmad, M. Abbas, I. Gunawan, R.A. Shakoor, F. Ubaid, F. Touati, Electro-sprayed PVA coating with texture-enriched surface morphology for augmented humidity sensing, Progress in Organic Coatings 117 (2018) 7–9, https://doi.org/10.1016/j.porgcoat.2017.12.010.
[50] W. Liu, L. Zhu, C. Huang, X. Jin, Direct Electrospinning of ultrafine fibers with interconnected macropores enabled by in situ mixing microfluidics, ACS Appl. Mater. Interfaces 8 (50) (2016) 34870–34878, https://doi.org/10.1021/acsami.6b11362.
[51] S. Park, K. Park, H. Yoon, J. Son, T. Min, G. Kim, Apparatus for preparing electrospun nanofibers: designing an electrospinning process for nanofiber fabrication, Polym. Int. 56 (11) (2007) 1361–1366, https://doi.org/10.1002/pi.2345, 10.1002/pi.2345 (acccessed 2022/03/07).
[52] R. Aflaha, H. Afiyanti, Z.N. Azizah, H. Khoirudin, A. Rianjanu, A. Kusumaatmaja, R. Roto, K. Triyana, Improving ammonia sensing performance of quartz crystal microbalance (QCM) coated with nanofibers and polyaniline (PANi) overlay, Biosensors Bioelectron. X 13 (2023) 100300, https://doi.org/10.1016/j.biosx.2022.100300.
[53] A. Rianjanu, M. Aulya, M.A.A.P. Rayhan, R. Aflaha, S. Maulana, T. Taher, W. S. Sipahutar, M.I. Maulana, N. Yulianto, K. Triyana, et al., Impact of hydrophilic bamboo cellulose functionalization on electrospun polyacrylonitrile nanofiber-based humidity sensors, MRS. Commun. 13 (3) (2023) 514–519, https://doi.org/10.1557/s43579-023-00367-w.
[54] R. Aflaha, L. Katriani, A.H. As'ari, N.L.I. Sari, A. Kusumaatmaja, A. Rianjanu, R. Roto, K. Triyana, Enhanced trimethylamine gas sensor sensitivity based on quartz crystal microbalance using nanofibers overlaid with maltodextrin, MRS. Commun. 13 (4) (2023) 664–672, https://doi.org/10.1557/s43579-023-00409-3.
[55] R. Aflaha, N.L.I. Sari, L. Katriani, A.H. As'ari, A. Kusumaatmaja, A. Rianjanu, R. Roto, H.S. Wasisto, K. Triyana, Maltodextrin-overlaid polyvinyl acetate nanofibers for highly sensitive and selective room-temperature ammonia sensors, Microchem. J. 193 (2023) 109237, https://doi.org/10.1016/j.microc.2023.109237.
[56] M. Febrina, A. Rianjanu, A. Rajak, R.R. Mukti, M. Djamal, Electrospun polyacrylonitrile nanofibers mixed with citric acid as a quartz crystal microbalance ammonia vapor sensor, ChemistrySelect. 7 (1) (2022) e202103615, https://doi.org/10.1002/slct.202103615.
[57] A. Rianjanu, K. Triyana, N. Nurbaiti, S.A. Hasanah, A. Kusumaatmaja, R. Roto, An enhanced safrole sensing performance of a polyacrylonitrile nanofiber-based-QCM sensor by overlaying with chitosan, Sains Malays 48 (9) (2019) 2041–2049, https://doi.org/10.17576/jsm-2019-4809-25.
[58] D.B. Nugroho, A. Rianjanu, K. Triyana, A. Kusumaatmaja, R. Roto, Quartz crystal microbalance-coated cellulose acetate nanofibers overlaid with chitosan for detection of acetic anhydride vapor, Results Phys. 15 (2019) 102680, https://doi.org/10.1016/j.rinp.2019.102680.
[59] C. Duan, Z. Zhang, X. Zhang, M. An, Y. Zhang, Y. Liu, M. Lu, High sensitivity and excellent durability of wearable microenvironmental humidity sensors inspired by the spider-web, Sens. Actuators, B 377 (2023) 133056, https://doi.org/10.1016/j.snb.2022.133056.
[60] S. Yu, H. Zhang, J. Zhang, Z. Hu, High-sensitivity RGO-TiO2 humidity sensor driven by triboelectric nanogenerators for non-contact monitoring of human respiration, J. Alloys Compd. 935 (2023) 168006, https://doi.org/10.1016/j.jallcom.2022.168006.
[61] G. Sauerbrey, Verwendung von Schwingquarzen zur Wägung dünner Schichten und zur Mikrowägung, Z. Physik 155 (2) (1959) 206–222, https://doi.org/10.1007/BF01337937.
[62] J. Xue, T. Wu, Y. Dai, Y. Xia, Electrospinning and Electrospun Nanofibers: methods, Materials, and Applications, Chem. Rev. 119 (8) (2019) 5298–5415, https://doi.org/10.1021/acs.chemrev.8b00593.
[63] M. Pakravan, M.-C. Heuzey, A. Ajji, A fundamental study of chitosan/PEO electrospinning, Polymer. (Guildf) 52 (21) (2011) 4813–4824, https://doi.org/10.1016/j.polymer.2011.08.034.
[64] P. Qi, Z. Xu, T. Zhou, T. Zhang, H. Zhao, Study on a quartz crystal microbalance sensor based on chitosan-functionalized mesoporous silica for humidity detection, J. Colloid Interface Sci. 583 (2021) 340–350, https://doi.org/10.1016/j.jcis.2020.09.029.
[65] C. Qiao, F.N. Bo, H.X. He, Y. Yao, J.Y. Rong, P. Wei, L. Dong, Humidity-sensing properties of a BiOCl-coated quartz crystal microbalance, ACS. Omega 5 (30) (2020). From Cnki.
[66] W. Hu, S. Chen, B. Zhou, L. Liu, B. Ding, H. Wang, Highly stable and sensitive humidity sensors based on quartz crystal microbalance coated with bacterial cellulose membrane, Sens. Actuators, B 159 (1) (2011) 301–306, https://doi.org/10.1016/j.snb.2011.07.014.
[67] Y. Li, Y. Chen, C. Zhang, T. Xue, M. Yang, A humidity sensor based on interpenetrating polymer network prepared from poly(dimethylaminoethyl methacrylate) and poly(glycidyl methacrylate), Sens. Actuators, B 125 (1) (2007) 131–137, https://doi.org/10.1016/j.snb.2007.01.048.
[68] X. Wang, B. Ding, J. Yu, M. Wang, Highly sensitive humidity sensors based on electro-spinning/netting a polyamide 6 nano-fiber/net modified by polyethyleneimine, J. Mater. Chem. 21 (40) (2011) 16231–16238, https://doi.org/10.1039/C1JM13037D, 10.1039/C1JM13037D.
[69] N. Horzum, D. Taşçıoglu, S. Okur, M.M. Demir, Humidity sensing properties of ZnO-based fibers by electrospinning, Talanta 85 (2) (2011) 1105–1111, https://doi.org/10.1016/j.talanta.2011.05.031.
[70] J. Lin, N. Gao, J. Liu, Z. Hu, H. Fang, X. Tan, H. Li, H. Jiang, H. Liu, T. Shi, et al., Superhydrophilic Cu(OH)2 nanowire-based QCM transducer with self-healing ability for humidity detection, J. Mater. Chem. A 7 (15) (2019) 9068–9077, https://doi.org/10.1039/c9ta01406c.
[71] H. Fang, J. Lin, Z. Hu, H. Liu, Z. Tang, T. Shi, G. Liao, Cu(OH)2 nanowires/graphene oxide composites based QCM humidity sensor with fast-response for real-

time respiration monitoring, Sens. Actuators, B 304 (2020) 127313, https://doi.org/10.1016/j.snb.2019.127313.
[72] A. Rianjanu, S.N. Hidayat, N. Yulianto, N. Majid, K. Triyana, H.S. Wasisto, Sensitivity prediction and analysis of nanofiber-based gas sensors using solubility and vapor pressure parameters, Jpn. J. Appl. Phys. 60 (10) (2021) 107001, https://doi.org/10.35848/1347-4065/ac1a8e.
[73] M.N. Pervez, W.S. Yeo, M.M.R. Mishu, M.E. Talukder, H. Roy, M.S. Islam, Y. Zhao, Y. Cai, G.K. Stylios, V. Naddeo, Electrospun nanofiber membrane diameter prediction using a combined response surface methodology and machine learning approach, Sci. Rep. 13 (1) (2023) 9679, https://doi.org/10.1038/s41598-023-36431-7.
[74] B. Han, T.H. Rupam, A. Chakraborty, B.B. Saha, A comprehensive review on VOCs sensing using different functional materials: mechanisms, modifications, challenges and opportunities, Renew. Sust. Energy Rev. 196 (2024) 114365, https://doi.org/10.1016/j.rser.2024.114365.
[75] K. Liao, F. Wang, Q. Shen, Y. Liu, Z. Mei, H. Wang, S. Zhang, S. Ma, L. Wang, Advances in humidity sensors based on Self-Powered technology, Chem.Eng. J. 505 (2025) 159480, https://doi.org/10.1016/j.cej.2025.159480.
[76] J. Qin, Y. Tang, Y. Zeng, X. Liu, D. Tang, Recent advances in flexible sensors: from sensing materials to detection modes, TrAC Trends Anal. Chem. 181 (2024) 118027, https://doi.org/10.1016/j.trac.2024.118027.
[77] G. Mu, Y. Zhang, Z. Yan, Q. Yu, Q. Wang, Recent advancements in wearable sensors: integration with machine learning for human–machine interaction, RSC. Adv. 15 (10) (2025) 7844–7854, https://doi.org/10.1039/D5RA00167F, 10.1039/D5RA00167F.